14th International Particle Accelerator Conference,Venice, Italy JACoW Publishing
ISBN: 978-3-95450-231-8 ISSN: 2673-5490 doi: 10.18429/JACoW-IPAC2023-THXD1

TOWARDS THE COXINEL SEEDED FREE ELECTRON LASER WITH A LASER PLASMA ACCELERATOR AT HZDR*

M. E. Couprie†, M. Labat, T. André, A. Berlioux, P. Berteaud, F. Blache, F. Bouvet, F. Briquez, C. de Oliveira, J. P. Duval, Y. Dietrich, M. El Ajjouri, C. Herbeaux, N. Hubert, C. Kitégi, S. Lê, B. Leluan, A. Loulergue, F. Marteau, M. H. N'guyen, D. Oumbarek-Espinos[1], D. Pereira, J. P. Ricaud, P. Rommeluère, M. Sebdaoui, K. Tavakoli, M. Valléau, M. Vandenberghe, J. Vétéran, Synchrotron SOLEIL, Saint-Aubin, France,
A. Ghaith, A. Irman, S. Bock, Y. Y. Chang, A. Debus, C. Eisenmann, R. Gebhardt, S. Grams, U. Helbig, M. Kuntzsch, M. La Berge, R. Pausch, T. Püschel, S. Schöbel, K. Steiniger, P. Ufer, U. Schramm, Helmholtz-Zentrum Dresden – Rossendorf, Dresden, Germany.
S. Corde, J. Gautier, J. P. Goddet, I. Andriyash, O. Kononenko, G. Lambert, V. Malka[2], P. Rousseau, A. Tafzi, C. Thaury,
LOA, ENSTA Paris, CNRS, Ecole Polytechnique, Institut Polytechnique de Paris, Palaiseau, France
E. Roussel Univ. Lille, CNRS, UMR 8523–PhLAM, Lille, France

Abstract

Developing Free Electron Lasers (FEL) using Laser Plasma Acceleration opens great hopes for compact laboratory scale light sources. The COXINEL line developed at Synchrotron SOLEIL (France), after having been installed at Laboratoire d'Optique Appliquée (France), has been moved to Helmholtz-Zentrum Dresden-Rossendorf (HZDR) (Germany) for using high-quality electron beam generated by the 150 TW DRACO laser. After proper electron beam transport, seed and undulator radiation temporal, spectral and spatial overlaps, the seeded Free Electron Laser driven by the DRACO laser plasma accelerator has been observed in the UV. Good agreement is found between measurements and simulations.

INTRODUCTION

Accelerator based light sources are nowadays knowing a very large development, serving for a variety of scientific investigations. Among them, Free Electron laser originates from the laser invention [1, 2], where the gain medium consists of relativistic electrons in the magnetic field of an undulator, leading under certain conditions to an electron bunching and coherent emission [3]. After the first infrared [4] and visible [5] FELs in the oscillator configuration, and coherent harmonic generation in the UV-VUV [6, 7], Self-Amplified Spontaneous Emission (SASE) was developed starting with long wavelengths [8]. FEL operation was then extended to shorter ones down to the X-ray range [9], thanks to high quality electron beams provided by photo-injectors and state-of-the-art accelerators, which performance have been updated in view of the next generation colliders. Longitudinal coherence is improved with external seeding [10] and self-seeding [11].

Laser Plasma Acceleration (LPA) concept [12] was also proposed after the laser discovery. An ultrashort and intense laser focused in a gas cell/jet excites a plasma oscillation, leading to a strong longitudinal accelerating field. High power lasers using chirped pulse amplification [13] boosted experimental demonstrations with hundred MeV range beams with few percent energy spread [14-16]. It opened the hope for driving FELs with LPA [17, 18] considering using a 5 fs- 1 PW laser leading to an LPA with 1.74 GeV, 0.1 % energy spread, 10 µrad divergence, 20 µm beam size, 1 nC charge and 150 kA peak current.

LPA experimental results kept progressing, reaching ~100 GV/m accelerating field with electron beams up to 8 GeV [19], 0.4%–1.2% energy spread [20], nC charge [21, 22], few fs bunch duration [23], and low emittance (~mm·mrad) [24]. These electron beam features, not simultaneously achieved, do not reach yet the ones currently achieved on conventional accelerators but they approach to what is needed for an FEL application with an adequate beam handling. Indeed, the first LPA based FEL has been demonstrated at SIOM with state-of-the-art LPA performance and three undulator segments at 27 nm in the SASE regime [25]. The second LPA driven FEL has been achieved on COXINEL (COherent X-ray source INferred from Electrons accelerated by lasers) at HZDR in the seeded configuration at 267 nm [26], enabling for an improved longitudinal coherence. After describing the design of COXINEL, its first preliminary results when installed at Laboratoire d'Optique Appliquée (LOA), the seeded FEL achieved at HZDR is presented.

COXINEL PREPARATION

COXINEL Design

Initial discussions between Laboratoire d'Optique Appliquée and Synchrotron SOLEIL for feasibility experiment to drive an FEL with LPA started in 2010. The COXINEL line was designed considering a 200 MeV electron beam with a 1 mrad RMS divergence, 1 µm RMS beam size, 3.3 fs RMS bunch length, 34 pC charge, 1% energy spread, 1 mm·mrad normalised emittance. In the line design, the 1 mrad divergence (as compared to a typical 100 µrad on conventional accelerator) is handled via a

† couprie@synchrotron-soleil.fr
[1] Present address: Osaka University, Japan.
[2] Present address: Weizmann Institute of Science, Israel

ISBN: 978-3-95450-231-8 ISSN: 2673-5490 doi: 10.18429/JACoW-IPAC2023-THXD1

strong transverse focusing [27, 28] right after the gas jet to avoid for emittance chromatic growth [29]. The large energy spread (1% as compared to typically 0.01% on conventional acceleration) is mitigated by a magnetic chicane: the slice energy spread is reduced by the chicane decompression factor and the bunch duration lengthens by the same factor, while the peak current decreases accordingly. One can take further advantage of the energy/position correlation introduced in the chicane to synchronize the electron beam transverse focusing with the light progress along the undulator, in the so-called "chromatic matching" regime [28]. The electron beam transport has been modelled including collective effects such as space charge and coherent synchrotron radiation [30]. FEL sensitivity to parameters has been studied [31]. The FEL features were analysed [32], showing a red-shifted FEL resulting from the chicane induced energy chirp coupled with undulator dispersion and fringes resulting from the inferences between the seed and the FEL, from which an FEL pulse reconstruction could be foreseen.

COXINEL Equipment

The so-called QUAPEVA quadrupoles designed for the strong focusing are built with permanent magnets enabling gradients up to 200 T/m with 50 % variability while maintaining the magnetic axis [33-35]. The chicane made of four electromagnetic dipoles powered by a Sigmaphi power supply reduces the energy spread and allows for the seed mirror insertion. An electromagnetic dipole dump is installed at the end of the chicane. Four electromagnetic quadrupoles located upstream the undulator are fed by 10 A power supplies from Sigmaphi. Four electromagnetic correctors are distributed along the line (after the LPA chamber, after the chicane, at undulator entrance and exit).

For going along with the compact LPA driving the FEL, short period high field undulators are preferred [36]. Three different 2-meter long undulators have been used for COXINEL: first the spare SOLEIL In Vacuum Undulator of 20 mm period (IVU20), replaced by the Cryogenic permanent Magnet Undulator of 18 mm period (CPMU18#2) operated at room temperature at LOA and then the IVU20#8 for the HZDR, since the CPMU18#2 was needed at SOLEIL [37, 38]. The magnetic field first harmonic B_u versus gap g fitted from the measurements $B_u = 2.58\exp[-3.37\ g + 0.095g^2]$ provides a maximum deflection parameter K_u of 2.47 at 4 mm minimum gap.

The COXINEL line is equipped with five motorized electron beam imagers at the exit of the LPA, at the chicane centre, at the entrance and exit of the undulator. The imagers consist of a scintillating screen, an imaging optics and a camera (Basler acA640 for the first one at LPA exit, HAMAMATSU, ORCA Flash 4.0 for the others), with resolutions of 150 μm for the first imager at the LPA exit, 4.7 μm in horizontal and vertical for the second imager located in the chicane for single shot emittance measurement, 6.0 (6.4) (resp. 6.5 (6.8)) μm in horizontal (vertical) at the undulator entrance (resp. exit) and 4.7 μm in horizontal and vertical for the beam dump imager. Turbo Integrating Current transformers (ICTs) from Bergoz, are located just after he LPA chamber and at the undulator exit [39]. The radiation is collected after the dipole dump by a plano-convex Fused Si of 40 cm focal length followed by plano-concave Fused Si of – 20 cm focal length. This optical set up enables to image the radiation along the undulator, either on an UV camera (Hamamatsu ORCA-II UV) or on a 2D spectrometer (Horiba/Jobin-Yvon iHR320) equipped with a CCD camera.

The different components have been prepared, pre-assembled with the mechanical and vacuum components and aligned on their specific girders [40-42].

COXINEL FIRST RESULTS AT LOA

Mastered Electron Beam Transport

The COXINEL line has been installed in February March 2016 and aligned in Salle Jaune at LOA. The 60 TW, 800 nm, 30 fs FWHM Ti:Sapphire laser is used for the LPA. Even though COXINEL was designed considering a colliding scheme [16], the LPA was operated mainly in the ionization injection scheme with the laser focused into a supersonic jet filled a gas mixture (99% Helium, 1% Nitrogen) with a focal spot of 12 × 15 μm^2 FWHM.

The electron beam generation is optimised and characterized with a first electron spectrometer, located 355 mm from the gas jet, consisting of a removable permanent magnet dipole (1.1 T field, 10 cm length) and a phosphor screen imaged on a CCD camera, providing a spectral resolution varying between 2.7 and 3.8% between 50 and 280 MeV. Electrons were generated with a broad energy spectrum. In 2017-2018, the typical slice vertical divergence measured on the spectrometer was typically of 3.5 mrad. The horizontal divergence is deduced from the vertical one, using a normalization factor measured on the first screen without QUAPEVAs.

The electron beam has been rapidly transported [43] but it appeared essential to motorize the QUAPEVAs under vacuum to insert or remove them for new characterization and readjustments of the electron beam. The first ICT that had initially been installed in the LPA generation chamber was moved downstream, out of the LPA chamber, to avoid false detection. In order to properly transport the electron beam and reproduce the expected electron beam profiles from the transport modelling with BETA [44], a beam-based alignment method was tried but the stability of the electron beam was not sufficient to get conclusive results. A Beam Pointing Alignment Compensation (BPAC) method was then developed, using the transfer matrix response of the line and the ability to move vertically and horizontally each QUAPEVA independently. Such a BPAC allows both the position and the dispersion of the electron beam to be adjusted independently [45]. An observed slight tilt on the beam image was attributed to skew quadrupolar components of the QUAPEVAs, that have been further corrected in the magnetic measurement laboratory [46, 47].

Shock injection [48] was also tested and appeared less stable, so ionization injection was preferred for first alignment steps. A slit was then inserted in the chicane to reduce the electron beam energy spread [49] in ionization

14th International Particle Accelerator Conference,Venice, Italy JACoW Publishing
ISBN: 978-3-95450-231-8 ISSN: 2673-5490 doi: 10.18429/JACoW-IPAC2023-THXD1

injection. Further improvements on the LPA tuning enabled to limit the divergence and improve the charge density.

Controlled Undulator Radiation

LPA based undulator radiation had been previously observed on different experiments [50-52]. On COXINEL, the transverse undulator radiation was first measured using several bandpass filters and compared to simulations [43]. Then, the undulator resonant wavelength was adjusted while varying the undulator gap [53]. The first harmonic spectral bandwidth was controlled by adjusting the energy spread via the slit located in the chicane, showing a good agreement with simulations of the beam transport and undulator radiation (with SRW code [54]) and analytical expressions.

FEL Search

In view of a seeded FEL demonstration, a seed was first prepared with High order Harmonics generated in Gas at 200 and 270 nm, and then with an EKSMA kit at 270 nm for easier operation out of vacuum. For FEL search, the electron and the seed were spatially overlapped by imaging in the undulator, spectrally tuned on the spectrometer, synchronised with a photodiode and then by spatial interference for the first attempts, and then with a Hamamatsu FESCA streak camera for the second trials. Despite the improvements after an upgrade of the laser, the electron beam quality with 1.5 mrad divergence and 1.5 pC/MeV was still too far from the baseline reference parameters and the seeded FEL demonstration could not be achieved at LOA.

COXINEL LINE INSTALLATION AT HZDR

Feasibility Studies and Preparation

The electron beam results achieved with the DRACO laser being close to the COXINEL baseline reference case, it was considered to move the line at HZDR in case of an unsuccessful FEL search at LOA. Feasibilities studies in 2020-2021 covered the adaptation to the infrastructure (see Fig. 1), new electron beam measurements at 200 MeV, the energy of interest for a seeded FEL at 270 nm on COXINEL, followed by the adjustment of the electron beam transport and FEL modelling with GENESIS [55]. The QUAPEVAs have been modified with Phytron motors for better vacuum compatibility. A new in-vacuum undulator has been built because the one used at LOA was needed for other purposes. A new server with an update version of TANGO was prepared. It was decided to move in September 2021.

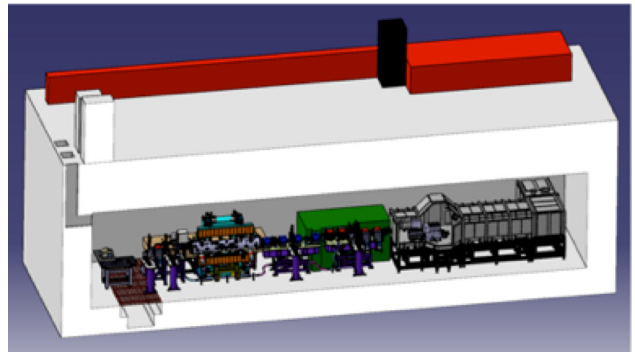

Figure 1: Implementation of the COXINEL line in HZDR LPA cave.

Line Transport and Installation

The line was transported and installed in the HZDR cave at the end of October 2021 (see Fig. 2), with members of different SOLEIL groups (mechanical engineering, vacuum, magnet and insertion devices, power supplies, diagnostics, alignment). The girders and the different equipment have been aligned with a theodolite and a laser tracker, taking the cross reference of the HZDR laser positions and fiducial references taken on the magnet measurement bench for the undulator.

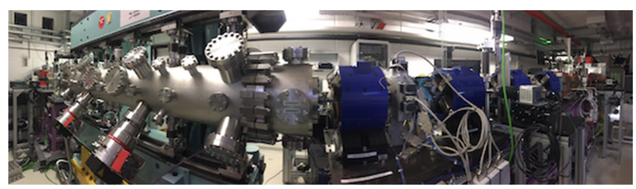

Figure 2: Picture of the COXINEL line installed in HZDR LPA cave.

HZDR ELECTRON BEAM

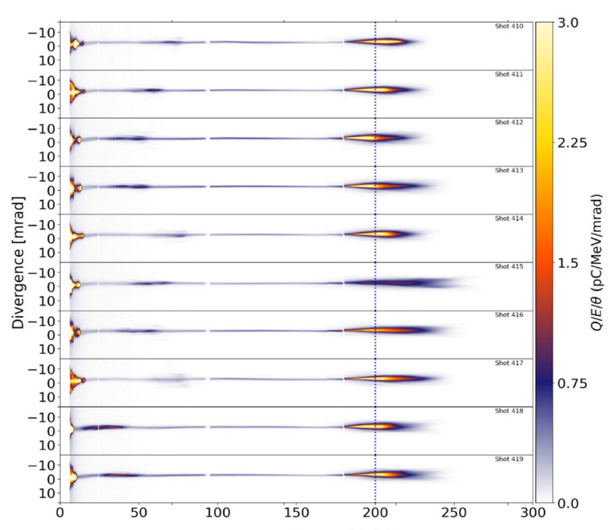

Figure 3: LPA e beam generated by the DRACO laser characterized on the magnetic spectrometer.

The LPA is operated with the 100 TW branch of the DRACO laser (30 fs FWHM, 2.1 J on target) in the tailored

ISBN: 978-3-95450-231-8 ISSN: 2673-5490 doi: 10.18429/JACoW-IPAC2023-THXD1

self-truncated ionization-induced injection [56] with 99 % He-1 % N_2 gas mixture. In such a configuration at 188 MeV, beam loading limits the energy spread to 6 % RMS [21] and shaping the gas density profile induces a passive plasma lens which provides moderate divergences (in the horizontal plane of 0.8 mrad), leading to 6.3 pC/MeV FWHM average charge density [26]. The electron bunch duration estimate is of 14.8 fs FWHM [23]. Successive spectra shown in Fig. 3 indicates the rather good stability of the facility, with small energy deviation from shot to shot.

COXINEL ELECTRON BEAM TRANSPORT AND SPONTANEOUS EMISSION AT HZDR

The envelops of the electron beam transport along the COXINEL line are shown in Fig. 4 for three different electron beam energies.

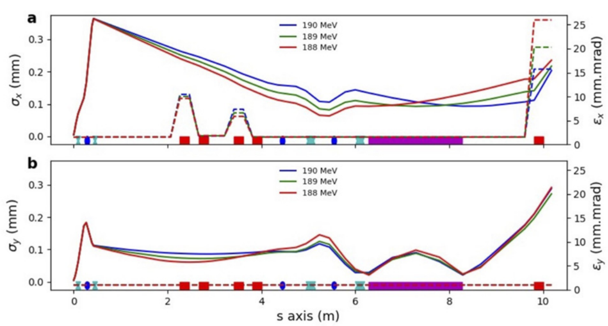

Figure 4: Electron beam envelops for different electron beam energies (ELEGANT simulations [57]).

Electron beam transport along the COXINEL line was carried out in December 2021 (see Fig. 5). Because of its limited energy spread as compared to previous measurements at LOA, the crossed shape on the electron beam imagers practically disappears. Up to 150 pC are measured onto the ICT located at the exit of the undulator.

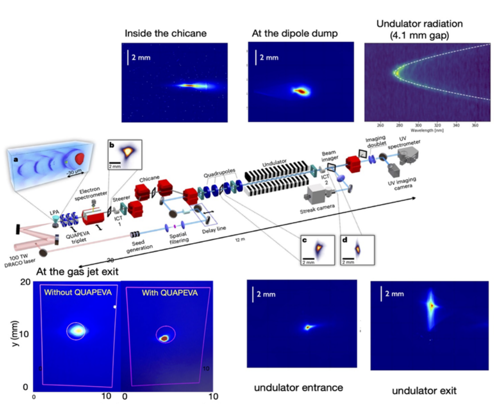

Figure 5: First electron beam transport of the HZDR LPA beam in COXINEL line (measured with the chromatic matching optics) and undulator radiation (measured with a slit optics with a slit close at 1 mm, leading to an energy spread of 0.9 % rms).

Undulator spontaneous emission was also measured, exhibiting the expected characteristics (as shown in Fig. 5).

COXINEL SEEDED FEL AT HZDR

The Seed Preparation at 269 nm

The seed has been prepared by the HZDR team. A small fraction of the LPA driver laser is frequency tripled (EKSMA femtokit) with a group velocity compensation. The seed is then spectrally and spatially filtered, and stretched to 1 ps FWHM. The seed has a 3.9 nm (FWHM) bandwidth. It is injected into the COXINEL line with an Al mirror. The measured energy is of 0.8 µJ at injection and of 0.5 µJ at the undulator exit.

Seed and Undulator Radiation Overlap

The seed and undulator radiation are spectrally tuned looking at their spectra on the iHR320 Horiba-Jobin Yvon spectrometer, spatially overlapped by imaging in the undulator on a Hamamatsu ORCA-II UV camera and temporally synchronised looking at the arrival times with a FESCA 100 Hamamatsu streak camera from HZDR.

Seeded FEL Evidence

First FEL search took place in February 2022. During the first delay scan, the FEL signal was observed, as shown in Fig. 6 [26]. The FEL is red-shifted, as expected [32].

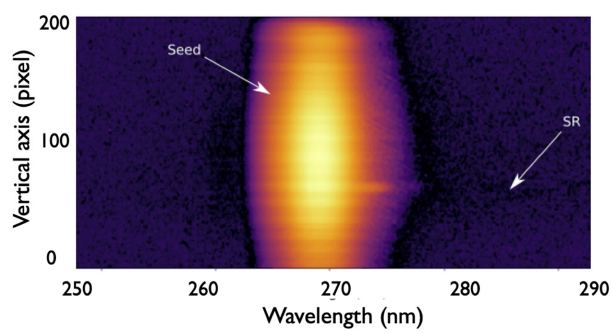

Figure 6: First seeded FEL signal measured on COXINEL at HZDR.

The FEL effect is confirmed by observing separately the seed, the spontaneous undulator radiation and the FEL. The measurements are in agreement with transport and radiation calculations using measured electron parameters at the source [26]. The quadratic charge dependence is confirmed [26]. Dependence versus delay [26] is also studied and compared to modelling: the red shift corresponds to the expectations from the simulations and analytic calculations [26, 32]. The dependence versus delay provides an additional wavelength tuning. The undulator gap dependence for wavelength tuning has also been checked. The expected fringes resulting from the phase-locked interference of the seed and the coherent are observed [26, 32], confirming the longitudinal coherence of the COXINEL seeded FEL at HZDR. The various measurements have been reconfirmed during another experimental session in Nov. 2022.

CONCLUSION

The first seeded FEL driven by a LPA is reported here in the UV [26]. Such a success results mainly from the quality of the HZDR LPA beams, following years on efforts on beam quality. Still, for reaching shorter wavelengths, further electron beam improvements are foreseen, paving the way for first pilot user experiments.

ACKNOWLEDGEMENTS

Authors thanks for the support from ERC (COXINEL (340015, PI: M.-E. Couprie), X-Five (339128, PI: V. Malka), M-PAC (715807, PI, S.Corde) , Fondation de la Coopération Scientifique (QUAPEVA-2012-058T), Laserlab Europe V (contract no. 871124), Helmholtz Association (programme Matter and Technology, topic Accelerator Research and Development), Germany's Federal Ministry of Education and Research (BMBF) (Verbundforschung LADIAG), METEOR CNRS Momentum grant (E. Roussel), CPER P4S, Agence Nationale de la Recherche (ANR DYNACO, ANR-DFG ULTRASYNC (ANR-19-CE30-0031), LABEX CEMPI ANR-11-LABX-0007).

REFERENCES

[1] A. L. Schawlow and C. H. Townes, "Infrared and Optical Masers", *Phys. Rev. Lett.*, vol. 112, p. 1940. 1958. doi:10.1103/physrev.112.1940

[2] T. H. Maiman, "Stimulated emission of radiation in ruby", *Nature*, vol. 187, p. 493. 1960. doi:10.1038/187493a0

[3] J. M. J. Madey, "Stimulated emission of Bremsstrahlung in a periodic magnetic field*", J. Appl. Phys*., vol. 42, p. 1906, 1971. doi:10.1063/1.1660466

[4] D. A. G. Deacon *et al.*, "First operation of a free-electron laser", *Phys. Rev. Lett.*, vol. 38, p. 892, 1977. doi:10.1103/physrevlett.38.892

[5] M. Billardon *et al.*, "Optical frequency multiplication by an optical klystron", *Phys. Rev. Lett.*, vol. 51, p. 1652, 2014. doi:10.1103/physrevlett.51.1652

[6] B. Girard *et al.*, "Optical frequency multiplication by an optical klystron", *Phys. Rev. Lett.*, vol. 53, p. 2405, 1984. doi:10.1103/physrevlett.53.2405

[7] R. Prazeres *et al.*, "Coherent harmonic generation in the vacuum ultraviolet spectral range on the storage ring ACO", *Nucl. Instrum. Methods*, vol. 272, p. 68, 1988. doi:10.1103/PhysRevLett.114.050511

[8] A. L. Throop *et al.*, "Experimental results of a high gain microwave FEL operating at 140 GHz", *Nucl. Instrum. Methods*, vol. 272, p. 15, 1988. doi:10.1016/0168-9002(88)90187-8

[9] P. Emma *et al.*, "First lasing and operation of an ångstrom-wavelength free-electron laser", *Nat. Photonics*, vol. 4, p. 641, 2010. doi:10.1103/PhysRevLett.114.050511

[10] L. H. Yu *et al.*, "High-gain harmonic-generation free-electron laser", *Science.*, vol. 289, no. 5, p. 5481, 2000. doi:10.1126/science.289.5481.932

[11] A. A. Lutman *et al.*, "Demonstration of single-crystal self-seeded two-color X-ray free-electron lasers", *Phys. Rev. Lett.*, vol. 113, no. 5, p. 254801, 2013. doi:10.1103/physrevlett.110.134801.

[12] T. Tajima and J. M. Dawson, *et al.*, "Laser electron accelerator", *Phy. Rev. Lett.*, vol. 43, p. 267, 1979. doi:10.1103/PhysRevLett.43.267

[13] D. Strickland and G. Mourou, "Compression of amplified chirped optical pulses", *Opt. Commun.*, vol. 55, p. 447, 1985. doi:10.1016/0030-4018(85)90151-8

[14] S. P. Mangles *et al.*, "Monoenergetic beams of relativistic electrons from intense laser-plasma interactions", *Nature.*, vol. 431, p. 535, 2004. doi:10.1038/nature02939

[15] C. G. R. Geddes *et al.*, "High-quality electron beams from a laser wakefield accelerator using plasma-channel guiding", *Nature.*, vol. 431, p. 538, 2004. doi:10.1038/nature02900

[16] J. Faure *et al.*, "A laser-plasma accelerator producing monoenergetic electron beams", *Nature.*, vol. 431, p. 541, 2004. doi:10.1038/nature02963

[17] F. Grüner *et al.*, "Design considerations for table-top, laser-based VUV and X-ray free electron lasers", *Appl. Phys. B*, vol. 86, p. 431, 2007. doi: 10.1007/s00340-006-2565-7

[18] K. Nakajima *et al.*, "Towards a table-top free-electron laser", *Nat. Phys.*, vol. 4, p. 92, 2008. doi: 10.1038/nphys846

[19] A. J. Gonsalves *et al.*, "Petawatt laser guiding and electron beam acceleration to 8 GeV in a laser-heated capillary discharge waveguide", *Phys. Rev. Lett.*, vol. 112, p. 084801, 2019. doi:10.1103/PhysRevLett.122.084801

[20] W. T. Wang *et al.*, "High-brightness high-energy electron beams from a laser wakefield accelerator via energy chirp control", *Phys. Rev. Lett.*, vol. 117, p. 124801, 2016. doi:10.1103/PhysRevLett.117.124801

[21] J. P. Couperus *et al.*, "Demonstration of a beam loaded nanocoulomb-class laser wakefield accelerator.", *Nat. Commun.*, vol. 8, p. 487, 2017. doi:10.1038/s41467-017-00592-7

[22] J. Götzfried *et al.*, "Physics of high-charge electron beams in laser-plasma wakefields", *Phys. Rev. Lett.*, vol. 114, no. 5, p. 050511, Feb. 1983. doi:10.1103/PhysRevLett.114.050511

[23] O. Zarini *et al.*, "Multioctave high-dynamic range optical spectrometer for single-pulse, longitudinal characterization of ultrashort electron bunches", *Phys. Rev. Accel. Beams*, vol. 25, p. 012801, 2022. doi:10.1103/PhysRevAccelBeams.25.012801

[24] G. R. Plateau *et al.*, "Low-emittance electron bunches from a laser-plasma accelerator measured using single-shot X-ray spectroscopy", *Phys. Rev. Lett.*, vol. 109, p. 064802, 2012. doi:10.1103/PhysRevLett.109.064802

[25] W. Wang *et al.*, "Free-electron lasing at 27 nanometres based on a laser wakefield accelerator", *Nature*, vol. 595, p. 516, 2021. doi:10.1038/s41586-021-03678-x

[26] M. Labat *et al.*, "Seeded free-electron laser driven by a compact laser plasma accelerator", Nature Photon., vol. 17, p. 150, 2022. doi:10.1038/s41566-022-01104-w

[27] M. E. Couprie *et al.*, "Towards a free electron laser based on laser plasma accelerators", Jour. Phys. B: At. Mol. Opt. Phys, vol. 47, no. 23, p. 234001, 2014. doi:10.1088/0953-4075/47/23/234001

[28] A. Loulergue *et al.*, "Beam manipulation for compact laser wakefield accelerator based free-electron lasers", *New Jour.*

ISBN: 978-3-95450-231-8 ISSN: 2673-5490 doi: 10.18429/JACoW-IPAC2023-THXD1

Phys., vol. 17, no. 2, p. 023028, 2015. doi:10.1088/1367-2630/17/2/023028

[29] K. Floettmann *et al.*, "Some basic features of the beam emittance", *Phys. Rev. Accel. Beams*, vol. 6, p. 034202, 2003. doi:10.1103/PhysRevSTAB.6.034202

[30] M. Khojoyan *et al.*, "Transport studies of LPA electron beam towards the FEL amplification at COXINEL", Nucl. Instr. Meth. A., vol. 829, p. 260, 2016. doi:10.1016/j.nima.2016.02.030i

[31] M. Labat *et al.*, "Robustness of a plasma acceleration based Free Electron Laser", Phys. Rev. Accel. Beams., vol. 21, p. 114802, 2018. doi:10.1103/PhysRevAccelBeams.21.114802

[32] M. Labat *et al.*, "Interferometry for full temporal reconstruction of laser-plasma accelerator-based seeded free electron lasers", New Journ. Phys., vol. 22, no. 1, p. 013051, 2020. doi:10.1088/1367-2630/ab6878

[33] C. Benabderrahmane, M. E. Couprie, SOLEIL, F. Forest, O. Cosson Sigmaphi, *et al.*, "Adjustable magnetic multipole", Patent Europe., EP 3189715 B1, Jun. 2018, https://bases-brevets.inpi.fr/fr/document/EP3189715/publications.html

[34] F. Marteau *et al.*, "Variable high gradient permanent magnet quadrupole (QUAPEVA),", Appl. Phys. Lett., vol. 111, p. 25, 2017. doi:10.1063/1.4986856

[35] A. Ghaith *et al.*, "Tunable high gradient quadrupoles for a laser plasma acceleration based FEL", Nucl. Instr. Meth. A., vol. 909, p. 290, 2018. doi:10.1016/j.nima.2018.02.098

[36] A. Ghaith *et al.*, "Undulator design for Laser Plasma Based Free electron laser", Phys. Rept., vol. 937, p. 2184, 2021. doi:10.1016/j.physrep.2021.09.001

[37] C. Benabderrahmane *et al.*, "Development and operation of a Pr2Fe14B based cryogenic permanent magnet undulator for a high spatial resolution x-ray beam line", Phys. Rev. Accel. Beams., vol. 20, p. 033201, 2017. doi:10.1103/PhysRevAccelBeams.20.033201

[38] M. Valléau *et al.*, "Development of Cryogenic Permanent Magnet Undulators at SOLEIL", Synchrotron Radiation News., vol. 31, no. 3, p. 42, 2018. doi:10.1080/08940886.2018.1460175

[39] M. Labat *et al.*, "Electron and photon diagnostics for plasma acceleration-based FELs"." *Journ. Synchrotron Rad.*, vol. 25, no. 1, p. 59, 2018. doi:10.1107/S1600577517011742

[40] M. E. Couprie *et al.*, "Towards free electron laser amplification to qualify laser plasma acceleration", *Rev. Laser Engineering.*, vol. 45, no. 2, p. 94, 2017. doi:10.1107/S1600577517011742

[41] M. E. Couprie *et al.*, "An application of Laser Plasma Acceleration: Towards a Free Electron Laser amplification", *Plasma Physics & Controlled Fusion.*, vol. 58, no. 3, p. 034020, 2016. doi:10.1088/0741-3335/58/3/034020

[42] M. E. Couprie *et al.*, "Towards a free electron laser using laser plasma acceleration on COXINEL", *Plasma Physics & Controlled Fusion.*, vol. 2054, no. 1, p. 030034, 2019. doi:10.1063/1.5084597

[43] T. André *et al.*, "First electron beam measurements on COXINEL", presented at the 7th Int. Particle Accelerator Conf. (IPAC'16), Busan, Korea, Jun. 2016, paper MOP0W005, unpublished.

[44] J. Payet *et al.*, "BETA code", *CEA-Saclay* 2015, http://irfu.cea.fr/Sacm/logiciels/index6.php

[45] T. André *et al.*, "Control of laser plasma accelerated electrons for light sources", *Nat. Comm.*, vol. 9, p. 1334, 2018. doi:10.1038/s41467-018-03776-x

[46] D. Oumbarek-Espinos *et al.*, "Skew quadrupole effect of laser plasma electron beam transport", *Appl. Sci.*, vol. 9, no. 12, p. 2447, 2019. doi:10.3390/app9122447

[47] D. Oumbarek-Espinos *et al.*, "COXINEL transport of laser plasma accelerated electrons", *Plasma Physics & Controlled Fusion.*, vol. 62, no. 3, p. 034001, 2020. doi:10.1088/1361-6587/ab5fec

[48] C. Thaury *et al.*, "Shock assisted ionization injection in laser-plasma accelerators", *Scient. Rep.*, vol. 5, p. 16310, 2015. doi:10.1038/srep16310

[49] E. Roussel *et al.*, "Energy spread tuning of a laser-plasma accelerated electron beam in a magnetic chicane", *Plasma Physics & Controlled Fusion*, vol. 62, no. 7, p. 074003, 2020. doi:10.1088/1361-6587/ab8ca0

[50] H. P. Schlenvoigt *et al.*, "A compact synchrotron radiation source driven by a laser-plasma wakefield accelerator", *Nat. Phys.*, vol. 4, p. 130, 2008. doi:10.1038/nphys811

[51] M. Fuchs *et al.*, "Laser-driven soft-X-ray undulator source", *Nat. Phys.*, vol. 5, p. 826, 2009. doi:10.1038/nphys1404

[52] M. P. Anania *et al.*, "An ultrashort pulse ultra-violet radiation undulator source driven by a laser plasma wakefield accelerator", *Appl. Phys. Lett.*, vol. 104, p. 264102, 2014. doi:10.1063/1.4886997

[53] A. Ghaith *et al.*, "Tunable high spatio-spectral purity undulator radiation from a transported laser plasma accelerated electron beam", *Sci. Rep.*, vol. 9, p. 19020, 2019. doi:10.1038/s41598-019-55209-4

[54] O. Chubar *et al.*, "A three-dimensional magnetostatics computer code for insertion devices", *J. Synchrotron Rad.*, vol. 5, p. 481, 1998. doi:10.1107/S0909049597013502

[55] S. Reiche *et al.*, "Genesis 1.3: a fully 3d time-dependent FEL simulation code", *Nucl. Instrum. Meth. A.*, vol. 429, no. 1-3, p. 243, 1999. doi:10.1016/S0168-9002(99)00114-X

[56] A. Irman *et al.*, "Improved performance of laser wakefield acceleration by tailored self-truncated injection", *Plasma Physics & Controlled Fusion*, vol. 60, p. 044015, 2018. doi:10.1088/1361-6587/aaaef1

[57] M. Borland, "Elegant: A flexible SDSS-compliant code for accelerator simulation", Argonne National Laboratory, 2000.